PROCEEDINGS OF SCIENCE

The impact of new estimates of models of stellar motion from VLBI on the alignment of the optically bright Gaia frame to ICRF3

Susanne Lunz,[a,b,*] **James M. Anderson,**[a,b] **Ming H. Xu,**[c,d] **Robert Heinkelmann,**[b] **Oleg Titov,**[e] **Jean-François Lestrade,**[f] **Megan C. Johnson,**[g] **Fengchun Shu,**[h] **Wen Chen,**[i] **Alexey Melnikov, Jamie McCallum,**[j] **Yulia Lopez,**[j] **Andrei Mikhailov, Pablo de Vicente Abad**[k] **and Harald Schuh**[a,b]

[a] *Technische Universität Berlin, Chair of Satellite Geodesy, Str. des 17. Juni 135, 10623 Berlin, Germany*
[b] *GFZ German Research Centre for Geosciences, Telegrafenberg, 14473 Potsdam, Germany*
[c] *Aalto University Metsähovi Radio Observatory, Metsähovintie 114, 02540 Kylmälä, Finland*
[d] *Aalto University Department of Electronics and Nanoengineering, PL15500, FI-00076 Aalto, Finland*
[e] *Geoscience Australia, PO Box 378, Canberra 2601, Australia*
[f] *Observatoire de Paris, LERMA, 77 avenue Denfert Rochereau, 75014 Paris, France*
[g] *United States Naval Observatory (USNO), 3450 Massachusets Ave NW, Washington, DC 20392, USA*
[h] *Shanghai Astronomical Observatory, 80 Nandan Road, Shanghai, 200030, China*
[i] *Yunnan Observatories, Yangfangwang 396th, Kunming 650011, Yunnan, China*
[j] *University of Tasmania,Private Bag 37, Hobart, Tasmania, 7001, Australia*
[k] *Observatorio de Yebes (IGN), Cerro de la Palera S/N, 19141, Guadalajara, Spain*

E-mail: susanne.lunz@gfz-potsdam.de

The reference frame determined by Gaia EDR3, Gaia-CRF3, is aligned to the International Celestial Reference System by referring to counterparts in its latest realization, the third International Celestial Reference Frame (ICRF3), which is calculated from very long baseline interferometry (VLBI) observations of extragalactic objects at radio frequencies. The objects in ICRF3, although bright at radio frequencies, are mostly faint at optical frequencies. The non-rotation of the optically bright Gaia frame to ICRF3 has to be tested separately because the Gaia dataset is known to be magnitude-dependent in terms of astrometric calibration. This can be done by identifying additional counterparts besides objects in ICRF3. Suitable counterparts are radio stars observed by VLBI relative to extragalactic objects in ICRF3 using phase-referencing. We discuss the rotational differences, i.e., orientation and spin, between the optically bright Gaia EDR3 and models of stellar motion from VLBI. In particular, we show the effects of improved models of stellar motion, for which we extended the time series from literature or archives with new VLBI results.

**** European VLBI Network Mini-Symposium and Users' Meeting (EVN2021) ****
**** 12-14 July, 2021 ****
**** Online ****

[*] Speaker

PoS(EVN2021)032

1. Testing the alignment of the Gaia bright frame

The Gaia satellite, operated by the European Space Agency (ESA), collects precise astrometric and photometric data of more than 1.8 billion objects at optical frequencies. The latest data release, Gaia EDR3, is based on the first 34 months of observational data [1]. The third realization of the International Celestial Reference Frame [ICRF3, 2] is a catalog of precise positions of 4 588 extragalactic radio sources at three different frequency setups, out of which 303 defining sources realize the orientation of the International Celestial Reference System (ICRS) axes. The ICRF3 was created based on a thorough analysis of almost 40 years of very long baseline interferometry [VLBI, 3] observations of the extragalactic, ideally point-like, objects by Earth-based radio antennas. These radio sources are typically bright at radio frequencies, but faint at optical frequencies. The celestial reference frame defined by Gaia data is aligned to the ICRF3 at S/X frequencies (which comprises 4536 radio sources) by a solid-body rotation onto the positions of the counterparts [4]. Ideally, the orientation offset $\boldsymbol{\epsilon(T)}$ between the two frames is zero, but more importantly the spin $\boldsymbol{\omega}$ is expected to be zero due to the non-rotation requirement of ICRF3[1].

As outlined in more detail in the appendix of [5], the alignment of the Gaia frame is magnitude dependent due to internal calibration procedures. Therefore, the non-rotation of calibration sections of visual magnitude G must be checked individually for their alignment to ICRF3. None of the 2269 counterparts between Gaia EDR3 and ICRF3 are brighter than $G \leq 13$ mag. For the bright Gaia DR2 frame ($G \leq 13$ mag) radio stars were collected from the literature and used for the alignment test in [5]. The stars are generally faint at radio frequencies and therefore can only be detected with a sufficient signal-to-noise ratio using the phase referencing method [6, 7], in which the star position is determined relative to a radio bright calibrator (ideally in ICRF3 S/X) based on phase delays. This is different from the approach of ICRF3, where quasar positions are adjusted along with other geodetic parameters based on group delays. [5] also suggested a mathematical approach that takes into account not only proper motions but also position offsets for the determination of the spin. A magnitude dependent weighting of the alignment was tested but not found to be unambiguously significant. Another approach was developed by [8], who used the proper motion differences between bright and faint stars in binaries and open clusters from Gaia EDR3 data alone to determine the spin. Their sample of 92 000 counterparts is significantly larger than the 41 counterparts in [5]. Therefore, it was possible to sort the counterparts into several bins of visual magnitude G, and a clear magnitude dependence of the alignment between faint and bright Gaia EDR3 frame was found. They report a spin of 40 μas yr^{-1} for the magnitude range $G \leq 10.5$ mag, and 80 μas yr^{-1} for the magnitude range 11 mag $\leq G \leq$ 13 mag. For both magnitude bands, the largest component is around the Y axis.

In this work, we evaluated the spin determination of Gaia EDR3 employing VLBI observations of radio stars as specified by [5], but with a homogenized and extended VLBI dataset. We tested two ways of extending the VLBI dataset with new star observations at one epoch. First, we produced absolute positions that are directly inserted into the spin determination. Second, we produced relative positions that were inserted into the time series of a star's relative positions whenever possible, with the goal of creating new estimates for models of stellar motion (position, proper motion, and parallax) whenever possible.

[1] Rotation is used as an umbrella term for orientation offset and spin.

2. Two different scenarios to the inclusion of new star positions

Data from the 41 stars as collected by [5] were homogenized by us so that all star positions refer to ICRF3 S/X whenever possible. Furthermore, one new position from phase-referencing with the VLBA was observed for 32 stars, seven of which were observed relative to two different phase-calibrators. Of the 32 stars, 18 were already included in the list of 41 stars. The frequency setup was chosen to be at X- or C-band, depending on the historic observations, to avoid any position shift in the precise relative position time series due to a possible frequency dependence of the star or calibrator position. The new positions were evaluated both as relative positions and as absolute positions with an appropriate realistic error budget as described in [9, submitted] and [10, submitted]. The relative positions are based on a fringe fit of the phase-calibrator with a source structure model applied, and the absolute positions are based on a corresponding fringe fit with a point source model applied, similar to ICRF3. Since compact calibrators were chosen, the differences between the two position types are mostly small, but the error budget is different.

Following the suggestion in [5], for the first scenario, denoted "55,EDR3,GA", the absolute positions were added to the homogenized data as single-epoch positions after correcting for the parallax effect and the Römer delay. The $\boldsymbol{\epsilon(T)}$ at the Gaia epoch $T = 2016.0$ and the $\boldsymbol{\omega}$ were determined from the position and proper motion differences between the VLBI and Gaia data propagated to the VLBI epoch. The Gaia parallaxes were corrected beforehand [11]. The residuals showed that outliers were present, so the star with the most deviating data was discarded and the calculation repeated. This rejection process was continued until the minimum number was reached for the rotation parameter adjustment. The result is a set of solutions for the rotation parameters with decreasing sample size. From these series, the weighted mean over all iterations (WM), the weighted root mean square of estimates around the WM (WRMS), and the mean formal error (ME) of each rotation parameter series were determined. We considered only solutions that are not affected by edge effects, such as too small number of stars or outlying stars still included. The same calculations were performed for a second scenario "55,EDR3,GA,NM" in which the new data for the 32 stars were not added directly as absolute one-epoch positions, but the relative positions were used to improve the estimates for the models of stellar motion. This was possible for 13 stars. For each of these stars, the input data was replaced with the new model estimates. Instead of the model position based on relative position measurements with phase-calibrator structure correction, the absolute position based on a point source fringe fit was used. In this way, the positions are connected to the ICRF3 in the best possible way, considering the given observations.

As shown in [10], for "55,EDR3,GA" the added WMs and the quadratically combined ME of $\epsilon(T)$ in X, Y, Z are 0.712 and 0.150 mas. The WM and ME of ω are 0.098 and 0.021 mas yr^{-1}. For "55,EDR3,GA,NM" the respective values are 0.780 and 0.175 mas resp. 0.106 and 0.019 mas yr^{-1}. "55,EDR3,GA,NM" has a higher $\epsilon(T)$ ME because fewer positions are involved in the adjustment since any multiple input for a star was replaced by the new model estimate and the absolute position. In contrast, its ω ME is smaller due to the more precise proper motion information from the new model estimates. They also result in a smaller quadratically combined ω WRMS (0.025 mas yr^{-1} and 0.021 mas yr^{-1}), while the $\epsilon(T)$ WRMS is slightly larger (0.124 mas and 0.147 mas). Applying a t-test (Behrens-Fisher problem, 5 % significance) to the individual rotation parameter series pairs shows that the estimates for $\epsilon_Y(T)$, ω_Y, and ω_Z are significantly different in the two scenarios.

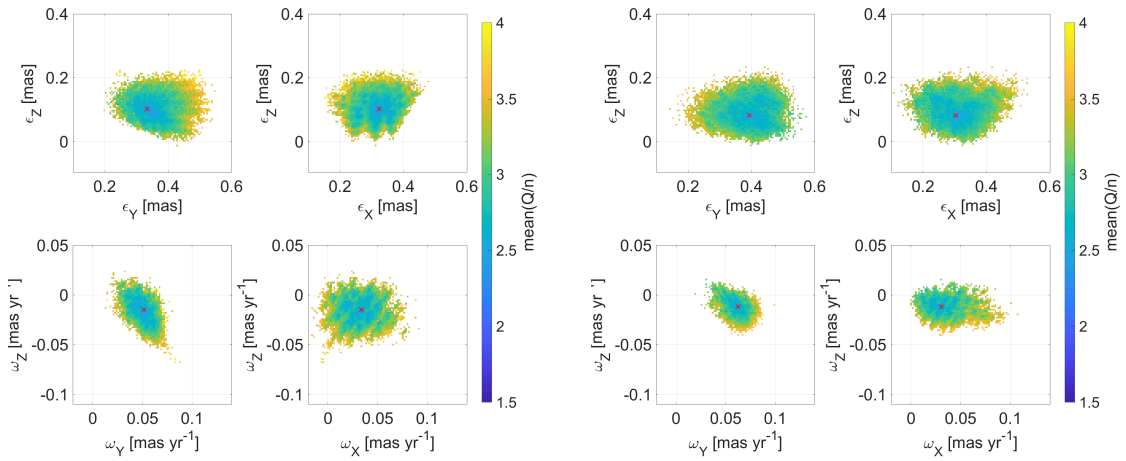

(a) WM for "55,EDR3,GA".

(b) WM for "55,EDR3,GA,NM".

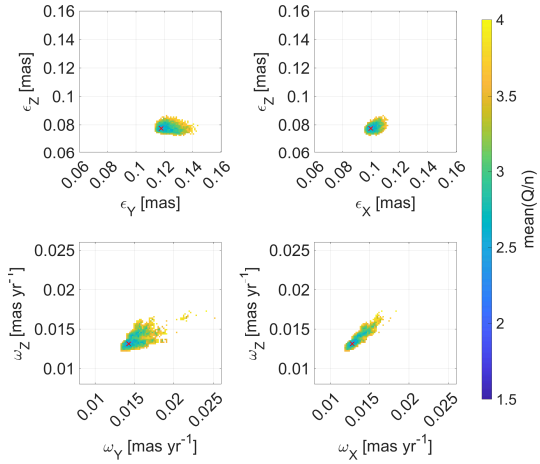

(c) ME for "55,EDR3,GA".

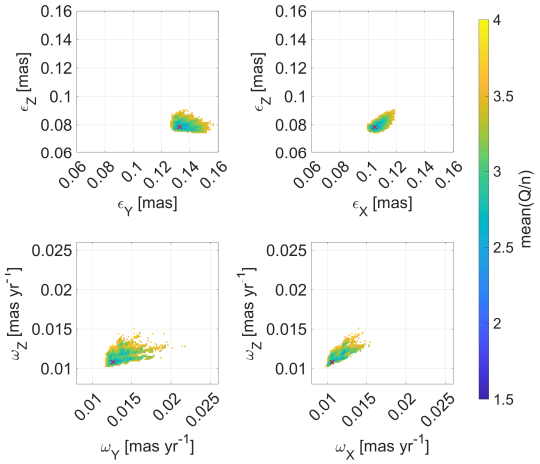

(d) ME for "55,EDR3,GA,NM".

Figure 1: WM and ME statistics of the rotations around the X, Y, and Z axes for the 163 185 individual scenarios based on the given scenario. The colors indicate the minimum value of the respective mean Q/n of its iterations, similar to the reduced χ^2, in each bin. In each of the subplots, the upper plots show the statistics for the orientation offset $\boldsymbol{\epsilon}(\boldsymbol{T})$ with $T = 2016.0$ and the lower plots for the spin $\boldsymbol{\omega}$. The red crosses label the solution with the minimum mean Q/n.

3. The accuracy of the alignment

For both scenarios, "55,EDR3,GA" and "55,EDR3,GA,NM", it was tested how much the rotation parameters diverge given only a small change in the sample of counterparts. To quantify the effect, the scatter of the WM, WRMS, and ME statistics was tested by running multiple solutions, where in each solution a unique combination of four stars was excluded. Furthermore, the same nine most divergent counterparts (typically due to non-linear proper motion) in each of the two scenarios were excluded a priori to not distort the statistics. This results in a total of 13 excluded stars and 163 185 possible solutions of each scenario. For each solution, the WM, WRMS and ME statistics were calculated from the rotation parameters of the first iteration to the 29th iteration. The scatter of the WM and ME statistics of the 163 185 solutions is shown in Figs. 1a and 1c for "55,EDR3,GA" and in Figs. 1b and 1d for "55,EDR3,GA,NM".

Comparing "55,EDR3,GA,NM" to "55,EDR3,GA", the scatter in $\boldsymbol{\omega}$ WM, the minimum $\boldsymbol{\omega}$ WRMS values, and the $\boldsymbol{\omega}$ ME values are smaller for "55,EDR3,GA,NM", while they gener-

Scenario		Min	Max	Mean
55,EDR3,GA	ϵ(**T**) [mas]	0.567	1.064	0.795
	ω [mas yr^{-1}]	0.018	0.183	0.102
55,EDR3,GA,NM	ϵ(**T**) [mas]	0.471	1.158	0.802
	ω [mas yr^{-1}]	0.041	0.194	0.110

Table 1: Minimum, maximum, and mean values of the added absolute WM_X, WM_Y, and WM_Z of the various solutions of scenarios "55,EDR3,GA" and "55,EDR3,GA,NM".

Scenario		ϵ(**T**) [mas]	ω [mas yr^{-1}]
55,EDR3,GA	WRMS	0.148	0.027
	ME	0.175	0.023
55,EDR3,GA,NM	WRMS	0.163	0.022
	ME	0.185	0.020

Table 2: Mean values of the quadratically combined WRMS and ME in X, Y, and Z of the various solutions of scenarios "55,EDR3,GA" and "55,EDR3,GA,NM".

ally increase for $\boldsymbol{\epsilon(T)}$. The scatter of the $\epsilon_Y(T)$ WRMS however is only half as large for "55,EDR3,GA,NM". The range of the added $\epsilon(T)$ WMs and ω WMs and its mean values for the various solutions are given in Table 1 for both scenarios. Also from these values, the range of $\epsilon(T)$ WM for "55,EDR3,GA" is smaller than for "55,EDR3,GA,NM", while for ω it is slightly larger. The improvement in spin determination is also supported by the quadratically combined mean values for WRMS and ME for both $\epsilon(T)$ and ω and both scenarios as presented in Table 2. If the distribution of the results of the rotation parameters is imagined as a histogram, the solutions group around the solution with the minimum sum of all Q/n of its iterations, where Q/n is equivalent to the reduced χ^2 of the solution.

From these values, it can be concluded that for the given data, adding new model estimates using the new relative positions improves the Gaia to VLBI spin determination more compared to adding the new data as absolute single-epoch positions. When formal errors are renormalized with $\sqrt{Q/n}$, the spin reaches a 3-σ significance in the Y-axis for solutions with low mean Q/n. The formal errors in Y are still less well determined compared to the other axes. The spin WM covers a wider range of values than the brightness dependent spin determined based on binaries and open clusters from the Gaia data itself in [8]. The estimates $(\omega_X, \omega_Y, \omega_Z) = (29.9 \pm 16.5, 63.1 \pm 19.7, -12.3 \pm 16.8)\,\mu\text{as yr}^{-1}$ from the solution with the lowest Q/n (2.4) in "55,EDR3,GA,NM" coincide with their spin in X and Y for $10.5 \leq G \leq 13$ and in Z for $G \leq 10.5$. More accurate and precise VLBI data, also of new counterparts, are needed to improve the alignment between radio and optical frames based on radio stars.

Acknowledgments

The authors acknowledge use of the Very Long Baseline Array under the US Naval Observatory's time allocation. This work supports USNO's ongoing research into the celestial reference frame and geodesy. We thank also the Socorro correlator for reliably and quickly providing the correlated data. The National Radio Astronomy Observatory is a facility of the National Science Foundation operated under cooperative agreement by Associated Universities, Inc. This project is supported by the DFG grants No. SCHU 1103/7-2, No. HE 5937/2-2, and SCHU 1103/26-1. M. H. Xu was supported by the Academy of Finland project No. 315721. This work has made use of the data from the European Space Agency mission Gaia processed by the Gaia Data Processing and Analysis Consortium. Funding for the DPAC has been provided by national institutions, in particular the institutions participating in the Gaia Multilateral Agreement.

References

[1] Gaia Collaboration, A. G. A. Brown, A. Vallenari, et al. (2021): A&A, 649 (2021) A1. doi:10.1051/0004-6361/202039657.
[2] P. Charlot, C. S. Jacobs, D. Gordon, et al. (2020): A&A, 644 (2021) A159. doi: 10.1051/0004-6361/202038368.
[3] H. Schuh and D. Behrend (2012): Journal of Geodynamics, 61 (2012) 68-80. doi: 10.1016/j.jog.2012.07.007.
[4] L. Lindegren, S. A. Klioner, J. Hernández, et al. (2020): A&A, 649 (2021) A2. doi: 10.1051/0004-6361/202039709.
[5] L. Lindegren (2020): A&A, 633 (2020) A1. doi: 10.1051/0004-6361/201936161.
[6] J. M. Wrobel, R. C. Walker, J. M. Benson, et al. (2012): https://library.nrao.edu/public/memos/vlba/sci/VLBAS_24.pdf.
[7] M. J. Reid and M. Honma (2014): Annual Review of Astronomy and Astrophysics, 52:1 (2014), 339-372. doi: 10.1146/annurev-astro-081913-040006.
[8] T. Cantat-Gaudin, T. D. Brandt (2021): A&A, 649 (2021) A124. doi: 10.1051/0004-6361/202140807.
[9] S. Lunz, J. M. Anderson, M. H. Xu, et al. (2020): Enhancing the link of the optically bright Gaia reference frame towards ICRS. submitted to A&A.
[10] S. Lunz, J. M. Anderson, M. H. Xu, et al. (2021): The impact of improved estimates of radio star astrometric models on the alignment of the *Gaia* bright reference frame to ICRF3. submitted to A&A.
[11] L. Lindegren, U. Bastian, M. Biermann, et al. (2021):A&A, 649 (2021) A4. doi: 10.1051/0004-6361/202039653.